Interface control of pressure-driven two-fluid flow in microchannels using electroosmosis

Wang, Cheng; Gao, Yandong; Nguyen, Nam-Trung; Wong, Teck Neng; Yang, Chun; Ooi, Kim Tiow

2005

Wang, C., Gao, Y. D., Nguyen, N. T., Wong T. N., Yang, C., & Ooi, K. T. (2005). Interface control of pressure-driven two-fluid flow in microchannels using electroosmosis. Journal of Micromechanics and Microengineering, 15(12), 2289-2297.

https://hdl.handle.net/10356/93881

https://doi.org/10.1088/0960-1317/15/12/011

Interface control of pressure-driven two-fluid flow in microchannels using electroosmosis

Cheng Wang, Yandong Gao, Nam-Trung Nguyen, Teck Neng Wong§, Chun Yang, Kim Tiow Ooi

† School of Mechanical and Aerospace Engineering, Nanyang Technological University, Nanyang Avenue 50, Singapore 639798

Abstract. This paper presents an experimental investigation of the pressure-driven two-fluid flow in microchannels with electroosmosis effect. Two fluids, aqueous NaCl solution and aqueous glycerol were introduced by syringe pumps to flow side by side in a straight microchannel. The external electric field was applied on the NaCl side. Under the same inlet volumetric flowrate condition, the applied electric field was varied. The interface position between the two fluids with the electroosmosis effect was studied in the first part of the experiment using fluorescence imaging technique. In the second part, the velocity field was measured using micro-PIV technique. The parameters, flowrate and electric field, which affect the interface position and velocity field were investigated. The measured velocity field from the experiment agrees well with that of theoretical analysis.

§ To whom correspondence should be addressed (mtnwong@ntu.edu.sg), Tel: (65) 67905587, Fax: (65) 67911895

1. Introduction

Manipulation of fluids in micro-scale is becoming more important as conventional lab can now be integrated into "a chip" [1]. Two-fluid flows in microchannel are often found in biological analysis, such as during ion exchange or solvent extraction from one phase to another phase [2]. In microfluidic devices, the Reynolds number is small and the flows are always laminar [3]. Laminar fluid diffusion interfaces (LFDIs) are generated when two or more streams flow in parallel within a single micro structure [4]. For laminar streams flowing side by side, diffusion is the only mechanism by which molecules can pass from one phase to another [5]. The diffusion through the phases is a function of diffusion coefficient and distance [6]. The mixing time is proportional to the square of the distance travelled. The mixing time can be reduced effectively by decreasing the diffusion distance. Many research studied on the ways to promote mixing in the small scale [7-9]. However, non-mixing in microchannels can be very useful as well. Because only diffusion occurs between different streams of flow, it is used for extraction or separation in the biological analysis [10, 11]. Diffusion-based microfluidic devices, such as the T-sensor® and the H-filter® have been developed for commercial use by Micronics, Inc [12]. In an extraction or separation of biological analysis, the two fluids used are biological fluid and aqueous reagent [13]. These two fluids usually have very different properties, such as density, surface tension and viscosity.

The variable viscosity of biological fluids can be problematic when the two streams of flow have different viscosities. The fluid with higher viscosity will spread wider in the channel while having a smaller velocity; whereas the fluid with lower viscosity flows at a larger velocity with a smaller fraction of the channel volume. These apply when the two flows have the same volumetric flow rate [4, 14]. The unmatched viscosity affects the diffusion in terms of the residence time. The average residence time of the more viscous fluid increases, while that of the less viscous fluid decreases. To overcome this problem, one of the methods is to measure the viscosity of the fluid, then add viscosity-enhancing solute to the less viscous fluid [13]. Another method called "flow-rate-ratio" is used to control the ratio of the volumetric flow rate of the two fluids [14]. By increasing the flow rate of the less viscous fluid, it is possible to maintain the interface of the two streams at the center position. However, the unmatched average residence time problem still remains unsolved, because the less viscous fluid flows faster and has a shorter average residence time within the channel.

Lee *et al* [15, 16] presented a multi-sample switch on a quartz substrate. The experimental data indicated that the multi-sample flows can be hydrodynamically pre-focused and guided into the outlet port based on the relative sheath and sample flow rate, i.e. the "flow-rate-ratio" method. It is noted that to achieve the desirable flow switching, flow ratio as high as 100 is required. Chein *et al* [17] proposed a numerical method to predict the flow switching phenomena under the controlled flow ratios. The result shows that, by changing the flow ratio between the buffer fluid and the sample fluid the interface position of the two streams varies. In addition, the flowrate ratio

required for the flow switching depends on the viscosity ratio of the fluids.

It is known that most solid surfaces acquire a certain amount of electrostatic charges when they are in contact with polar liquids, and hence a difference in potential is developed across the interface between the two phases. The charged interface attracts ions of opposite charge (counter-ion) and repels ions of like charge (co-ions) in the liquid. The arrangement of charges that occurs near the interface leads to the development of electric double layer (EDL) [18]. When a tangential electric field is applied along the capillary, liquids are pumped due to electroosmosis flow (EOF). Literature shows that the EOF principle has been widely used in micro-fluid pumping for the single fluid [19-25] and the "flow-rate-ratio" method has been applied to deliver multi-sample fluids in microfluidics [15-17]. Few of the previous studies integrate the EOF principles in the pressure-driven two-fluid flow, i.e. the combining effect of pressure gradient and electroosmosis in microfluidics. Until recently, theoretical work was done by Gao *et al* [26] to investigate the pressure-driven two-fluid flow with electroosmosis effect in microchannels.

This paper presents an experimental study of the pressure-driven two-fluid flow in an H-shaped microstructure with electroosmosis effect. In the first part of the experiment, the interface position between the two fluids, aqueous NaCl and aqueous glycerol, was investigated by fluorescence imaging technique. It demonstrated an alternative solution to control interface position for two fluids flow in microchannel. Secondly, the velocity profile measurement of the two fluids was carried out using micro-PIV techniques. The velocity field was measured quantitatively to study the electroosmosis effect. The parameters, volumetric flow rate and electric field, which affect the electroosmosis effect were discussed.

2. Experiment

2.1. Material and fabrication

The H-shaped microchannel used in the experiments is shown in Figure 1. The fabrication is based on the adhesive lamination techniques [27]. In this method, two polymethylmethacrylate (PMMA) plates (75 mm × 25 mm) are bonded by a layer or layers of double-sided adhesive tapes to form a closed microfluidic channel with inlet and outlet holes. The channel structure was cut through the adhesive tape (Arclad 8102 transfer adhesive, Adhesives Research Inc.). Thus the adhesive tapes define the depth of the channel. The two fluids flow side by side in the straight microchannel in the direction from the left to the right (E to F) by the syringe pump. A and C are the inlets for the two fluids; B and D are the outlets for collection of the products or wastes. Between A and B, platinum electrodes (Adrich-Sigma, Singapore) were inserted for the application of the electric field.

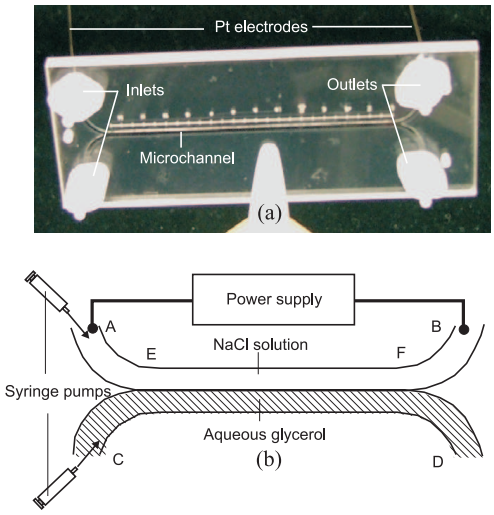

Figure 1. H-shaped microchannel: (a) the fabricated device used in the experiment; (b) schematic drawing of the channel configuration (the main channel is between E and F with a cross section of 910 μm $\times$ 100 μm), in which two fluids flow side by side (electric field from A to B: +ve, from B to A: -ve).

2.2. Experimental setup

A schematic of the experimental setup is shown in Figure 2. The setup can be used for both fluorescence imaging and micro-PIV measurement. It consists of four main components: an illumination system, an optical system, a coupled charge device (CCD) camera and a control system. The control system consisting of a peripheral component interface (PCI) card, and its corresponding software, is implemented in a personal computer (PC). The PC can control and synchronize all actions related to illumination and image recording.

Two different light sources were used for the two measurements. For the fluorescence imaging measurement, a single mercury lamp was used for illumination. Because of the ability of precise timing and intensity control, a laser beam was used for the micro-PIV (micro particle image velocimetry) measurement. In our system, a double pulsed Q-switched (quality switched) Nd:YAG laser was used. By including a Q-switch inside the cavity the laser can work in a triggered mode. The laser has a wavelength of 532 nm and a maximum energy of 160 mJ. The two-laser-head system allows the realization of two laser pulses with a very small delay. The system can work in different modes: single exposure in one frame, double exposure in one frame, and double exposure in double frames. In our experiments, the mode of double exposures in double frames was used because of the high signal-to-noise ratios and the better quality of the cross-correlation technique.

The optical system was a Nikon inverted microscope (Model ECLIPSE TE2000-S) with a set of epi-fluorescent attachments. There are three optical elements in a filter cube: excitation filter, dichroic mirror and emission filter. Emission filters are used in

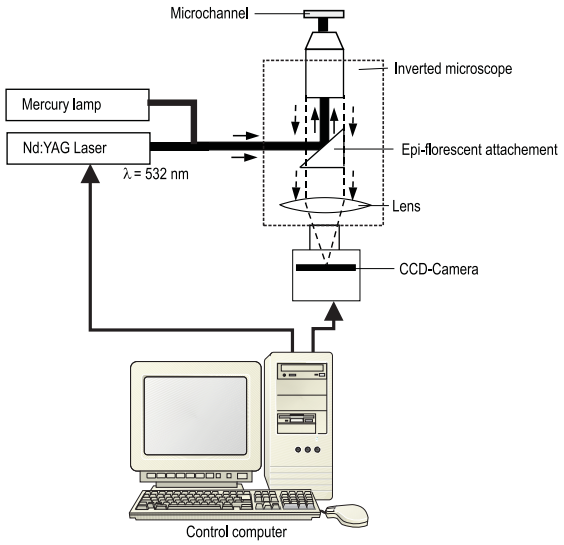

Figure 2. Schematic of the experimental setup for fluorescence imaging and micro-PIV measurements.

both measurements to select more specifically the emission wavelength of the sample and to remove traces of excitation light.

An interline transfer CCD camera (Sony ICX 084) was used for recording the images. The resolution of the camera is 640 pixels × 480 pixels, with 12 bits grayscale. The active area of the CCD sensor is 6.3 mm × 4.8 mm. The minimum inter-frame transfer time, and thus the fastest time delay for the two PIV images, is 300 ns. To ensure that the CCD camera is working at its optimum temperature of -15 °C , a cooling system is integrated in the CCD camera. In the mode of double exposure in double frames, the camera can record two frames of the flow fields and then digitizes them in the same image buffer.

3. Results and discussion

3.1. Fluorescence imaging measurement

For the study of interface position between the two fluids, a microchannel with the cross section of 910 μm × 100 μm and the length of 5 cm was used. The aqueous NaCl solution (concentration 7×10^{-4} M) and aqueous glycerol (volume concentration 14%) were introduced at inlets A and C through syringes (500 μL gastight, Hamilton) and syringe pump (Cole-Parmer, 74900-05, 0.2 L/h to 500 L/h, accuracy of 0.5%) system. The same volumetric flow rates of the two inlet flows were ensured by using two identical syringes driven by the syringe pump.

Fluorescent dye (fluorescein disodium salt $C_{20}H_{10}Na_2O_5$, also called Acid Yellow 73) was added in the NaCl solution for the purpose of image collection. When the fluoresein was illuminated by a mercury lamp, an epi-fluorescent attachment of type Nikon B-2A was used (excitation filter for 450-490 nm, dichroic mirror for 505 nm and an emission

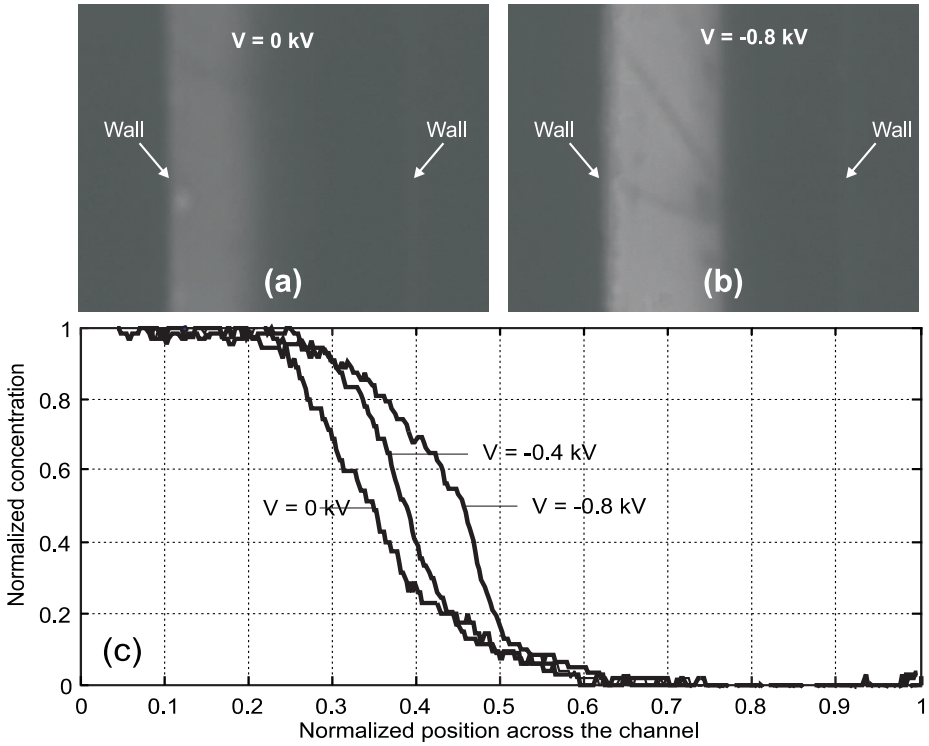

Figure 3. Measurement results at flow rate of 0.6 mL/h: (a) no electric field, NaCl solution holdup is about 35%; (b) under -0.8 kV, NaCl solution holdup is about 47%; (c) normalized concentration distribution of the fluorescent dye across channel width under different applied voltages.

filter for 520 nm) to record the fluorescent image. After recording the images, the interface position between the two fluids was determined by a customized algorithm written in a MATLAB program [27]. The algorithm removes the noise in thecollected images with an adaptive noise-removal filter, anddetermines the dimensionless pixel intensity across the channel.The dimensionless pixel intensity I^* is defined as,

$$I^* = \frac{I - I_{min}}{I_{max} - I_{min}} \tag{1}$$

where I_{max} and I_{min} are the maximum intensity and minimum intensity respectively.

A proportional relationship is assumed between the light intensity and the concentration of the fluorescent dye [28]. There exists aninter-diffusion region between the two fluids, because the twofluids are miscible. Gaussian distribution is assumed the diffusionof dye at the interface. By taking the derivative of concentration$c$ with respect to the distance x, the MATLAB program takes theposition where dc/dt is at its maximum as the interfaceposition. The typical images taken in the experiment and the concentration profiles are shown in Figure 3.

Because the two fluids in our experiment are both aqueous based solutions and miscible, a planar surface between NaCl solution and aqueous glycerol is assumed. The schematic is shown in Figure 4. The widths occupied by NaCl solution and aqueous

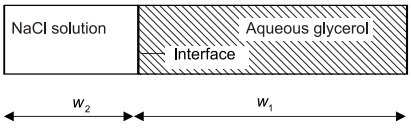

Figure 4. Cross sectional view of the two fluids in the main channel.

glycerol are denoted as w_2 and w_1. The holdup of NaCl e_2 is defined as the ratio of the area occupied by NaCl to the whole area of the cross-section of the channel, given as

$$e_2 = \frac{w_2 h}{(w_1 + w_2)h} = \frac{w_2}{w_1 + w_2} \tag{2}$$

Similarly, the holdup of the aqueous glycerol is

$$e_1 = 1 - e_2 \tag{3}$$

When the two fluids are in contact with the channel wall, a negatively charged surface potential is developed, which in turn influences the free ions distribution in the NaCl solution to form an electrical double layer (EDL) nearby the channel wall [18]. But for the aqueous glycerol, the EDL can hardly form due to the fact that few free ions are available. The conductivity of pure glycerol is 0.064 μS/cm at temperature 25 °C, while the conductivity of the NaCl solution (7×10^{-4} M) is about 86.6 μS/cm [29]. Thus the electroosmosis effect will only affect the NaCl solution flow. When a positive electric field is applied between A and B (A as the positive electrode, B as the negative electrode), the electroosmotic force will drag the NaCl solution to facilitate its flow in the same direction as the pressure-driven flow. If the negative electric field is applied (A is negative, B is positive), an opposite electroosmotic flow will be resulted, which, is against the pressure driven flow.

The parameters studied in the experiments are inlets volumetric flow rates and electric voltage applied between A and B. For different operating conditions, the measurement was taken when steady state conditions achieved. The holdup of the NaCl solutionwas obtained by normalizing its width to the whole channel width, according to Equation 2. As shown in Figure 5(a), as the electric field changes in magnitude and direction, the holdup of NaCl solution changes accordingly. When no voltage is applied across A and B, the flow is simply a pressure-driven two-fluid flow. The aqueous glycerol used is more viscous than NaCl solution, about 1.5 times. The less viscous NaCl solution occupies a smaller portion of the channel under pressure driven condition. The holdup value is about 0.35 when no externally applied voltage is present, as shown in Figure 5(a). When a negative electric field is applied across A and B, the holdup of NaCl solution increases. The electroosmotic flow is against the pressure-driven flow under a negative electric field. More resistance force will be encountered to drive the NaCl solution. The NaCl solution is flowing at a smaller velocity dueto the electroosmotic effect, thus occupies a larger channel width. The holdup of NaCl solution increases with the increase of negative electric field. Due to the same pressure drop across E and F, in order to achieve the same volumetric flow rates, the fluid which flows at a slower velocity

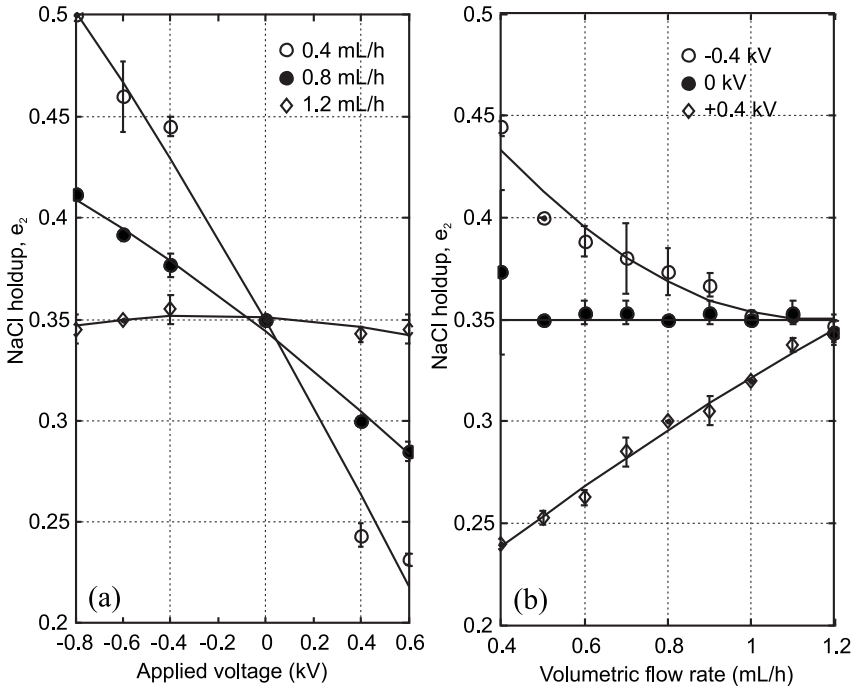

Figure 5. Relationship between NaCl solution holdup and (a) different applied voltage for the same volumetric flow rates of the two fluids or (b) volumetric flow rate under the same applied voltage.

has to spread to a larger width, i.e. a higher liquid holdup. In another case where the positive electric field is applied, the electrolyte solution NaCl is flowing faster, since the electroosmotic flow is in the same direction with the pressure-driven flow. Inanother words, electroosmotic effect aids the flow of the NaCl solution.

Figure 5(a) also shows that, as the inlet volumetric flowrates of the two fluids increase, the electroosmotic flow effect on the pressure-driven flow becomes weaker. At the flowrate of 1.2 mL/h, it seems that the holdup of NaCl, e_2 remains constant though the voltage varies from -0.8 kV to 0.6 kV. For typical electroosmotic flows, in which hundreds of volts per centimeter of the electric field is applied, the resulting velocity is of order 0.1 to a few mm/s. But for the pressure-driven flow in microchannels, the velocity can be controlled in a wider range. In this experiment, when the flow rate is at 0.4 mL/h, the average velocity of NaCl through the channel is 3.48 mm/s with no external applied electric field, the magnitude of which is comparable with that from the electroosmotic flow [30]. Figure 5(a) shows that by adjusting the electric field the interface position between the two fluids, i.e. variation of the NaCl holdup, from 0.25 to 0.50, has been successfully controlled.

The relationship between the NaCl holdup, e_2, at different flowrates under the fixed electric field is shown in Figure 5(b). The NaCl holdup e_2 remains the same (0.35) for different volumetric flowrates in the absence of an externally applied electric field. This is because the volumetric flow rates ratio between the two fluids is kept unchanged,

1:1. This agrees very well with the previous theoretical and numerical study reported in the literature [14]. From Figure 5(b), it can be seen that as flowrate increases, holdup e_2 converges to a constant value, 0.35 that is the value without the externally applied electric field. The reason is that larger pressure driven flow velocity makes the EOF effect almost insignificant.

3.2. Micro-PIV measurement

In our experiments, the seeding particles used were Duke red particles (Duke scientific Co.). The particles have a maximum excitation wavelength of 540 nm (green, very close to the characteristic wavelength of Nd: YAG) and a maximum emission wavelength of 610 nm (red). The diameter of the particles can be chosen from several hundreds of nanometers to several microns. The PIV-measurement uses an epi-fluorescent attachment of type Nikon G-2E/C (excitation filter for 540 nm, dichroic mirror for 565 nm and an emission filter for 605 nm). Both filters in the attachment have a bandwidth of 25 nm.

The measurement reported in this experiment was carried out with a 4× objective lens. We used a 640 × 480 CCD camera with square pixels 2.475 μm on the size. Fluorescent particles with a diameter of 3 μm were used to trace the flow. A microchannel with the cross section of 910 μm × 50 μm and the length of 5 mm was used. The fluids used in the experiment were the aqueous NaCl solution (concentration 10^{-4} M) and aqueous glycerol (volume concentration 24%). The fluorescent particles were diluted in the two fluids. Two 30 mJ laser pulses with a delay time of 3.5 ms were used as illumination sources. In our evaluation of velocity fields, double correlation method was used. The interrogation area is 32 pixels × 32 pixels. Previous studies show that the entry length of two fluids flow in microchannel was very short [27, 31]. The measurement was taken at 1mm downstream of the entrance, thus the stable velocity field was obtained.

The total measured velocity of the fluorescent tracing particle is a superposition of the electroosmotic, pressure-driven and electrophoretic and Brownian motion velocity components [32]. It can be expressed as

$$u_{particle} = u_{eof} + u_{pressure} + u_{eph} + u_b \tag{4}$$

where u_{eph} is the electrophoresis velocity of the tracing particle and u_b is the velocity due to Brownian motion of the particle. The electrophoresis velocity is a function of the particle's surface zeta potential in the solution [33], expressed as

$$u_{eph} = \frac{\varepsilon E_x \zeta_p}{\mu} \tag{5}$$

where ζ_p is the particle's surface zeta potential, and ε and μ is the permittivity and the dynamic viscosity of the fluid. In this experiment, the particle's zeta potential is -25.2 mV, which was measured by Yan [34]. From Einstein's Brownian movement

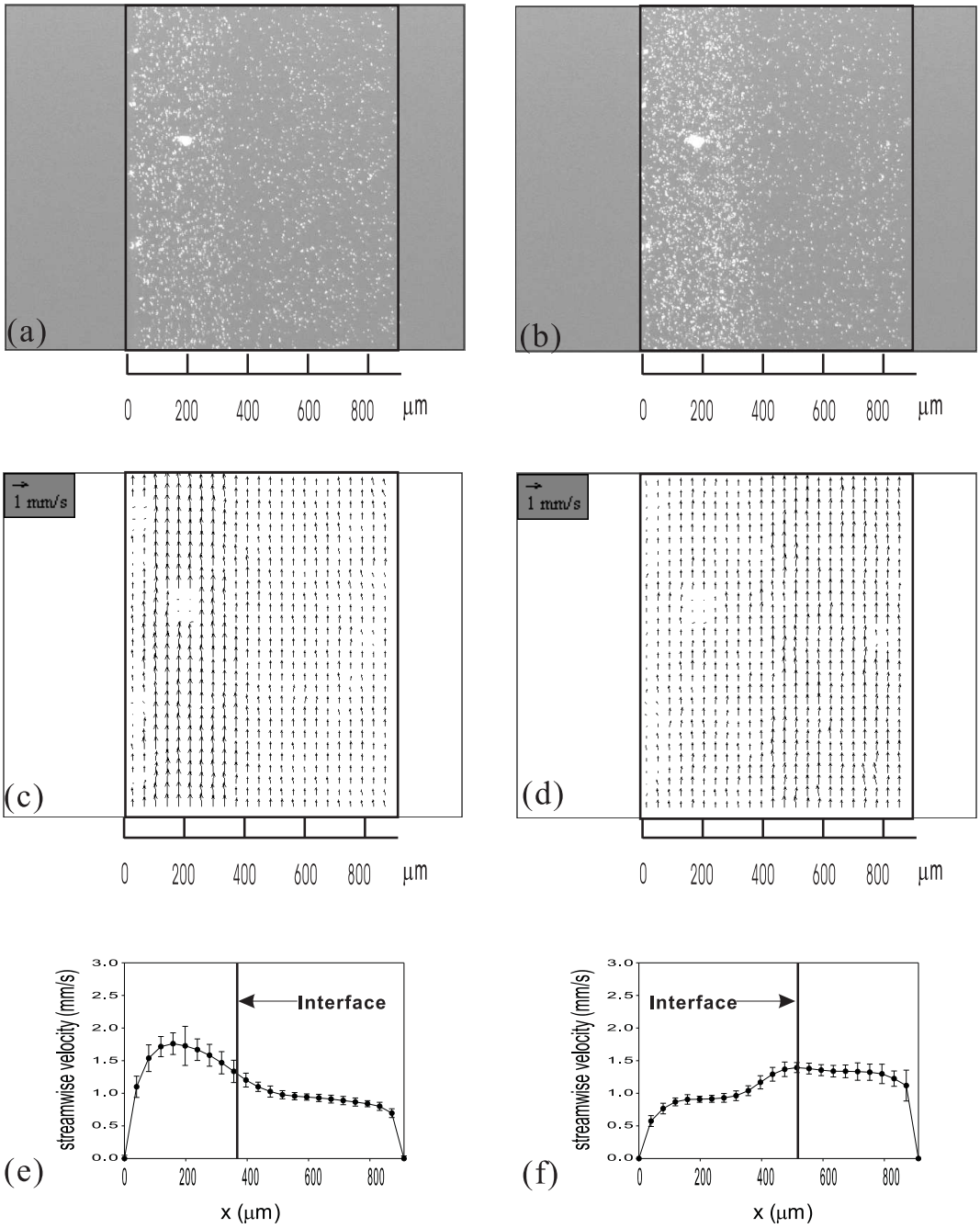

Figure 6. Micro-PIV measurements for 0.1 mL/h flow rate under different electric fields, (a) PIV image in absence of external electric field; (b) PIV image under -1.0 kV voltage electric field; (c), (d) the corresponding vector plots of the velocity field, (e), (f) the corresponding streamwise velocity profile over the channel width.

equation [35], the average Brownian velocity during the elapsed time duration between two subsequent images can be estimated as

$$u_b = \sqrt{\frac{2D}{\Delta t}} \tag{6}$$

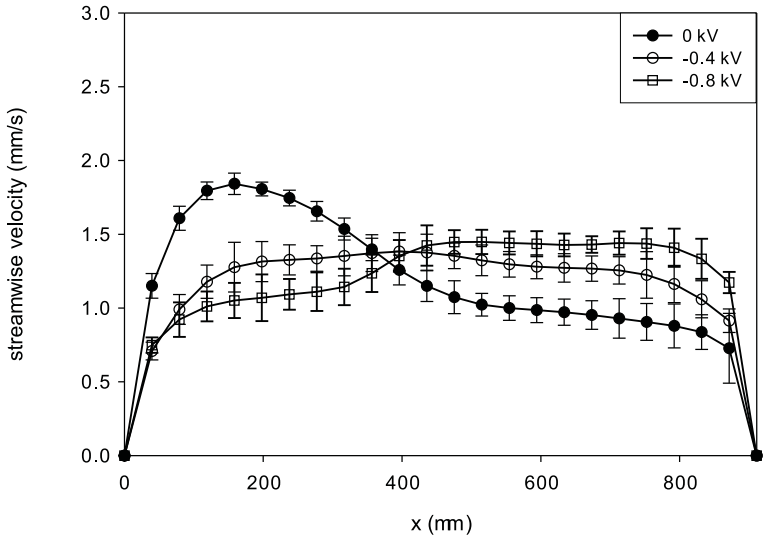

Figure 7. Velocity profile under different applied voltage (flow rate= 0.1mL/h, NaCl on left side, glycerol on right side in the Figure).

where Δt is the elapsed time duration and D is the diffusivity of the particles. The diffusivity is given by [36],

$$D = \frac{kT}{3\pi\mu d_p} \tag{7}$$

where T is the absolute temperature, k is the Boltzmann's constant and d_p is the particle diameter.

Figure 6 shows two typical results of the micro-PIV measurements, the inlet flowrates for NaCl and glycerol are 0.1mL/h for both inlets. The original images are shown in Figure 6(a), without the externally applied electric field and Figure 6(b) at applied voltage -1.0 kV. The respective vector plots of the velocity field are shown in Figure 6(c) and Figure 6(d). The corresponding streamwise velocities across the channel are shown in Figure 6(e) and Figure 6(f) respectively.

Figure 6(e) shows that in the absence of applied electric field, the less viscous fluid, NaCl, flows faster as the flowrates ratio between the two fluids is kept at 1:1. Figure 6(f) shows that the velocity of NaCl solution was decreased due to the electroosmosis effect which induced electroosmotic flow against the pressure-driven flow. The NaCl solution flows slower due tothe retarding of the electroosmosis effect, hence the average residence time of NaCl was longer than that of the aqueous glycerol. By adjusting the magnitude of voltage applied, the same average residence time for NaCl and glycerol can be achieved, i.e. the same average velocity for the two fluids.

The effect of the applied voltage is shown in Figure 7. Without the externally applied voltage, the NaCl (on the left side in Figure 7) flows faster. When a negative electric field is present, the velocity of NaCl decreases whereas the velocity of aqueous

glycerol increases. It is noted that as the applied voltage is set to -0.4 kV, both fluids have achieved about the same velocity, hence the same average residence time. If the applied voltage continues to increase to -0.8 kV, the NaCl flows at smaller velocity and spreads more in the channel. As the magnitude of the applied voltage increases, the interface position shift increases. This is in agreement with the fluorescent experiment observation.

To investigate the effect of electroosmosis under different flowrates, the dimensionless streamwise velocity profiles are presented in Figure 8. The dimensionless velocity at each measurement point is given as

$$U_i = \frac{u_i}{\frac{1}{N}\sum u_i} \tag{8}$$

where u_i is the velocity at the ith measurement point, N is the number of measurement points across the channel width. The dimensionless position X is normalized to the channel width, as

$$X = \frac{x}{w} \tag{9}$$

where x is position of the measurement point, w is the channel width. The velocity profile for different flow rates, 0.08 mL/h and 0.15 mL/h, are compared under the same externally applied electric field, of 0 kV in Figure 8(a), -0.2 kV in Figure 8(b), -0.6 kV in Figure 8(c) and -1.0 kV in Figure 8(d). The dimensionless velocity profile was obtained by normalizing the velocity to the average velocity through the channel. The results show that electroosmosis effect on the pressure-driven flow becomes significant as the inlet volumetric flowrates of the two fluids decreases. This agrees well with the experimental data on the interface position change with inlet flowrates as reported in Figure 5(b).

3.3. Comparison of theoretical analysis and micro-PIV measurement

In theoretical analysis [37], the electric potential in the conducing fluid, e.g. NaCl, is described by Poisson-Boltzmann equation, which can be written in terms of dimensionless variables as

$$\nabla^2\bar{\psi} = K^2\bar{\psi} \tag{10}$$

where $K = L\kappa$ is the ratio of the length scale L to the characteristic double layer thickness $1/\kappa$. Here κ is the Debye-Hückel parameter.

$$\kappa = \left(\frac{2z_0^2e^2n_0}{\varepsilon_r\varepsilon_0k_bT}\right)^{1/2} \tag{11}$$

in which ε_r is the relative permittivity of the conducting liquid and ε_0 is the permittivity of a vacuum. Once the electric potential distribution is known, the ionic net charge density due to zeta potential can be obtained through the relationship

$$\bar{\rho}^e = -2\bar{\psi} \tag{12}$$

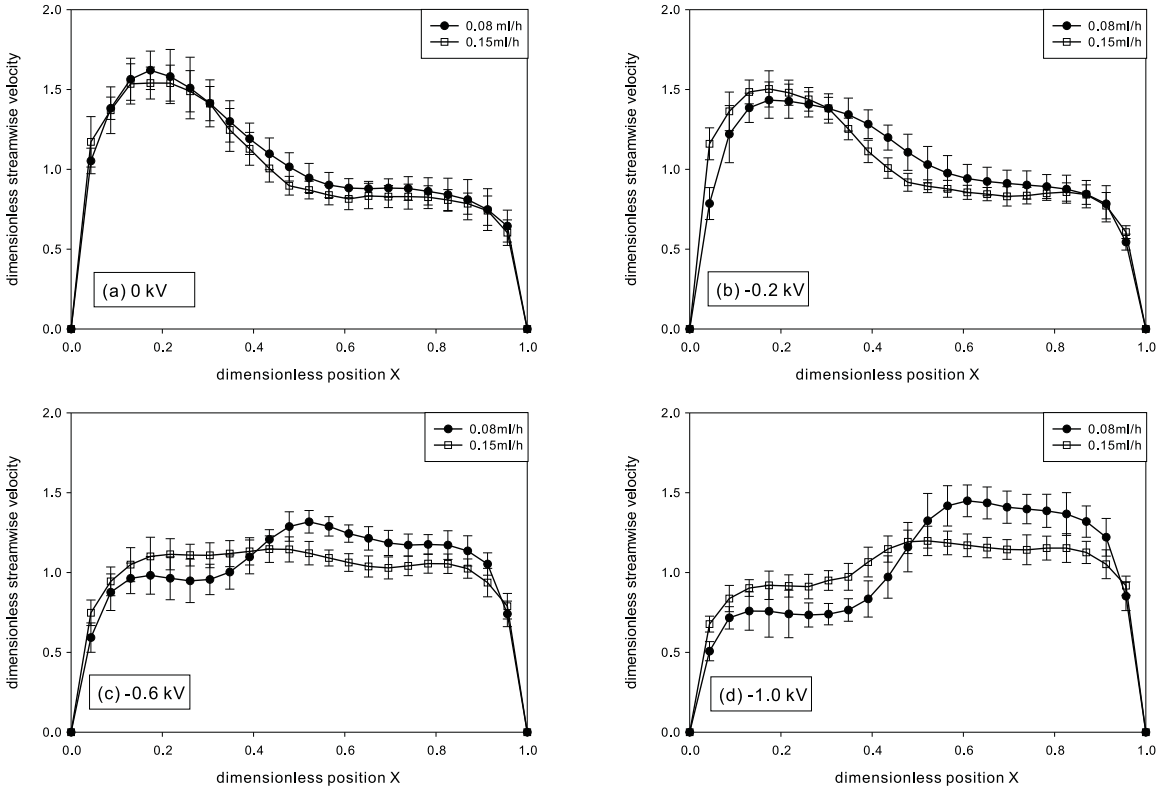

Figure 8. Dimensionless streamwise velocity profile for 0.08 mL/h and 0.15 mL/h under different applied electric field: (a) no electric field; (b) -0.2 kV voltage; (c) -0.6 kV voltage; (d) -1.0 kV voltage.

When an external electric field, E_x, is applied, the external electric filed interacts with these net charges within the double layers and creates an electroosmotic body force on the bulk of the conducting liquid. We assume that the two liquids are Newtonian and incompressible, and the flow is fully developed, the momentum equation for the conducting liquid gives

$$\nabla^2 \bar{u}_1 = \mathrm{Re}\frac{\mathrm{d}\bar{p}}{\mathrm{d}\bar{\mathrm{x}}} - S\bar{\rho}^e \tag{13}$$

where $\frac{\mathrm{d}\bar{p}}{\mathrm{d}\bar{\mathrm{x}}}$ is a constant dimensionless pressure gradient of the two liquids in the fully developed state, S is a parameter [38], which measures the relative importance of the electrical forces on the liquid flow

$$S = \frac{2z_0 e n_0 L^2 E_x}{\mu_1 V} \tag{14}$$

For the non-conducting fluid, the momentum equation gives

$$\nabla^2 \bar{u}_2 = \frac{\mathrm{Re}}{\beta}\frac{\mathrm{d}\bar{p}}{\mathrm{d}\bar{\mathrm{x}}} \tag{15}$$

where $\beta = \mu_2/\mu_1$ is the dynamic viscosity ratio. The boundary conditions are no-slip at channel wall. Additionally, at the interface matching conditions have to be obeyed, i.e.

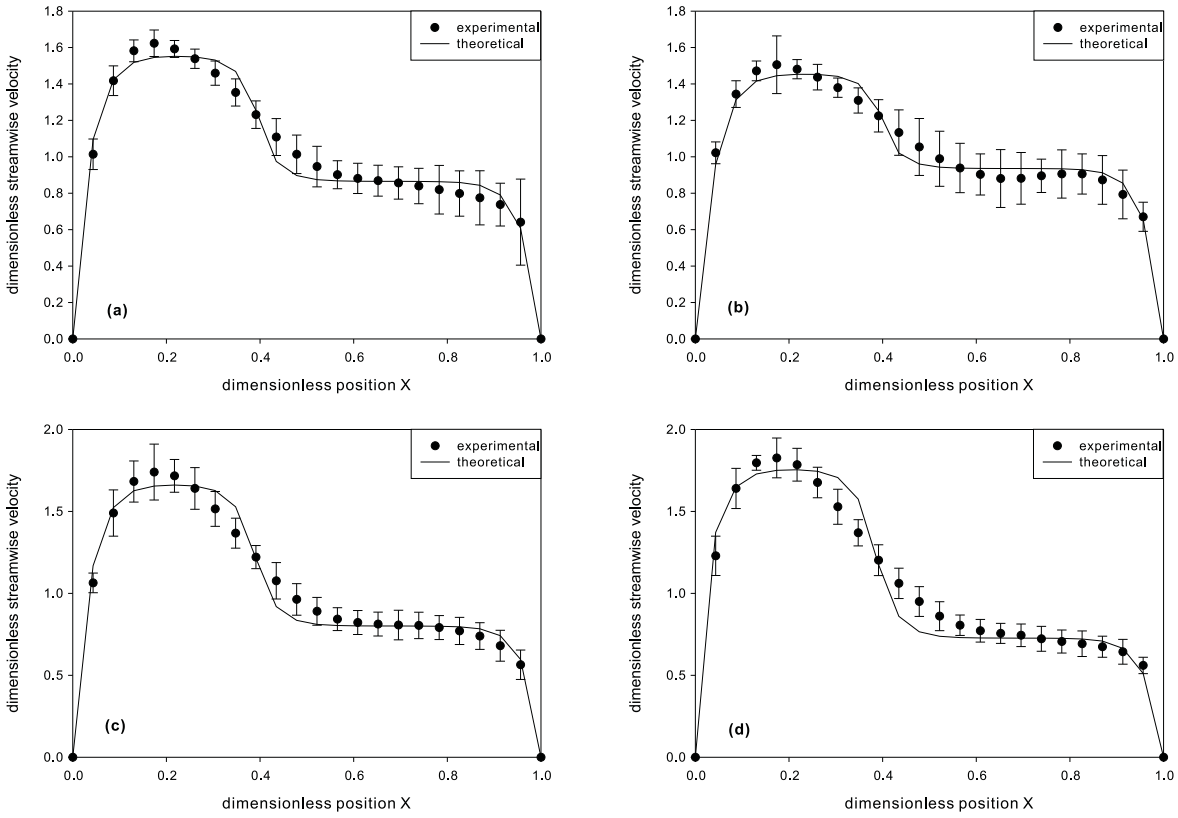

Figure 9. Comparison between PIV measurements and theoretical analysis at flow rate 0.1 mL/h, under various applied electric voltage. (a) no applied electric voltage, (b) -0.2 kV, (c) +0.2 kV and (d) +0.4 kV.

continuities of velocity and hydrodynamic shear stress,

$$\bar{u}_1 = \bar{u}_2 \tag{16}$$

$$\frac{\partial \bar{u}_1}{\partial y} = \beta \frac{\partial \bar{u}_2}{\partial y} \tag{17}$$

Because of the linearity, the velocity fields of conducting liquid and non-conducting liquid can be decomposed into two parts,

$$\bar{u}_1 = \bar{u}_1^E + \bar{u}_1^P \tag{18}$$

$$\bar{u}_2 = \bar{u}_2^E + \bar{u}_2^P \tag{19}$$

where the superscript E denotes velocity components due to electroosmotic forces, the superscript P denotes velocity components duet to the pressure gradient. Using the separation of variables method, the velocity by the electroosmotic force [37] and by the pressure gradient [39] can be obtained. The comparison between experiment and theoretical analysis under different applied electric field is shown in Figure 9. Reasonable agreement is obtained. In the theoretical prediction, a relatively sharp transverse

velocity gradient occurs at the interface as the model assumes two immiscible liquids. In fact, glycerol is miscible in water; therefore, there exists an interfacial region in the measured velocity profiles.

4. Conclusions

Our paper reports a new technique for controlling the velocity mismatch between two parallel fluid streams in a microchannel being driven by a pressure gradient. Because of the difference in viscosity of the two fluids, the more viscous fluid tends to occupy more width of the microchannel, thus cause the interface position deviation from the central position and residence time difference. This is problematic for diffusion-based microfluidic applications. The interface position of two-fluid flow in microchannel can be controlled using the electroosmosis effect, rather then the conventional "flow-rate-ratio" method. By applying electric potential along the microchannel, the electroosmosis effect retards or adds the flow of one stream, so that the velocity profile and interface position can be adjusted. The experiment demonstrated a new method to solve the unmatched viscosity problem of the two-fluid flow in microchannel, which are very often used in biological extraction or separation, sorting, or exchange process. Quantitatively, the velocity field of two-fluid under pressure and electroosmosis effect was measured using the micro-PIV technique. Comparison between theoretical prediction and the measured velocity profiles are presented.

Acknowledgments

This work was partially supported by the academic research fund of the Ministry of Education Singapore, contract number RG11/02. Cheng Wang gratefully acknowledges the Master of Engineering scholarship from the Nanyang Technological University.

References

[1] Knight, J. *Nature* **2002**, 418, 474-475.
[2] Kuban, P., Dasgupta, P. K., Morris, K. A. *Anal. Chem.* **2002**, 74, 5667-5675.
[3] Nguyen, N.-T., Wereley, S. T. *Fundamentals and applications of microfluidics*, Artech House: Boston, MA, 2002.
[4] Weigl, B. H., Bardell, R. L., Kesler, N., Morris, C. J. *Fresenius Journal of Analytical Chemistry* **2001**, 371, 97-105.
[5] Kamholz, A. E., Weigl, B. H., Finlayson, B. A., Yager, P. *Anal. Chem.* **1999**, 71, 5340-5347.
[6] Bird, R. B., Stewart, W. E., Lightfoot, E. N. *Transport phenomena*, 2nd ed., J. Wiley: New York, 2002.
[7] Burghelea, T., Segre, E., Bar-Joseph, I., Groisman, A., Steinberg, V. *Physical Review E* **2004**, 69, 066305.
[8] Chang, C. C., Yang, R. J. *Journal of Micromechanics and Microengineering* **2004**, 14, 550-558.
[9] Song, H., Bringer, M. R., Tice, J. D., Gerdts, C. J., Ismagilov, R. F. *Appl. Phys. Lett.* **2003**, 83, 4664-4666.

[10] Hisamoto, H., Horiuchi, T., Tokeshi, M., Hibara, A., Kitamori, T. *Anal. Chem.* **2001**, 73, 1382-1386.
[11] Dasher, R. B. *International Journal of Technology Management* **2002**, 23, 788-812.
[12] See *http://www.micronics.net/technologies/*
[13] Hatch, A., Garcia, E., Yager, P. *Proceedings of the Ieee* **2004**, 92, 126-139.
[14] Stiles, P. J., Fletcher, D. F. *Lab Chip* **2004**, 4, 121-124.
[15] Lee, G. B., Hung, C. I., Ke, B. J., Huang, G. R., Hwei, B. H. *Journal of Micromechanics and Microengineering* **2001**, 11, 567-573.
[16] Lee, G. B., Hwei, B. H., Huang, G. R. *Journal of Micromechanics and Microengineering* **2001**, 11, 654-661.
[17] Chein, R. Y., Tsai, S. H. *Biomedical Microdevices* **2004**, 6, 81-90.
[18] Hunter, R. J. *Zeta potential in colloid science : principles and applications*, Academic Press: London, 1981.
[19] Zeng, S. L., Chen, C. H., Mikkelsen, J. C., Santiago, J. G. *Sensors and Actuators B-Chemical* **2001**, 79, 107-114.
[20] Chen, C. H., Santiago, J. G. *Journal of Microelectromechanical Systems* **2002**, 11, 672-683.
[21] Lazar, I. M., Karger, B. L. *Anal. Chem.* **2002**, 74, 6259-6268.
[22] Pu, Q. S., Liu, S. R. *Anal. Chim. Acta* **2004**, 511, 105-112.
[23] Yao, S. H., Santiago, J. G. *J. Colloid Interface Sci.* **2003**, 268, 133-142.
[24] Yao, S. H., Hertzog, D. E., Zeng, S. L., Mikkelsen, J. C., Santiago, J. G. *J. Colloid Interface Sci.* **2003**, 268, 143-153.
[25] Tripp, J. A., Svec, F., Frechet, J. M. J., Zeng, S. L., Mikkelsen, J. C., Santiago, J. G. *Sensors and Actuators B-Chemical* **2004**, 99, 66-73.
[26] Gao, Y., Wong, T. N., Yang, C., Ooi, K. T. *Journal of Colloid and Interface Science* **2005**, 284, 304-316.
[27] Wu, Z., Nguyen, N.-T., Huang, X. *Journal of Micromechanics and Microengineering* **2004**, 14, 604-611.
[28] Sato, Y., Irisawa, G., Ishizuka, M., Hishida, K., Maeda, M. *Meas. Sci. Technol.* **2003**, 14, 114-121.
[29] Yaws, C. L., Knovel (Firm) *Yaws' handbook of thermodynamic and physical properties of chemical compounds physical, thermodynamic and transport properties for 5,000 organic chemical compounds*, Knovel: Norwich, N.Y., 2003.
[30] Geschke, O., Klank, H., Tellemann, P. *Microsystem engineering of lab-on-a-chip devices*, Wiley-VCH ,: Weinheim, 2004.
[31] Kim, B. J., Liu, Y. Z., Sung, H. J. *Meas. Sci. Technol.* **2004**, 15, 1097-1103.
[32] Devasenathipathy, S., Santiago, J. G., Takehara, K. *Anal. Chem.* **2002**, 74, 3704-3713.
[33] Probstein, R. F. *Physicochemical hydrodynamics : an introduction*, 2nd ed., John Wiley & Sons: New York, 1994.
[34] Yan, D.*Unpublished PhD candicate first year technical report* **2004**.
[35] Einstein, A. *Investigations on the theory of the Brownian movement*, Dover Publications: New York, 1956.
[36] Friedlander, S. K. *Smoke, dust, and haze : fundamentals of aerosol behavior*, Wiley: New York, 1977.
[37] Gao, Y., Wang, C., Wong, T. N., Yang, C., Nguyen, N.-T., Ooi, K. T. **2005**, *submitted to Lab On a Chip.*
[38] Cox, R. G. *J. Fluid Mech.* **1997**, 338, 1-34.
[39] Churchill, S. W. *Viscous flows : the practical use of theory*, Butterworths: Boston, 1988.